HYDROLOGICAL PROCESSES
Hydrol. Process. **18**, 1871–1884 (2004)
Published online 12 May 2004 in Wiley InterScience (www.interscience.wiley.com). DOI: 10.1002/hyp.1453

Observations on the movement of coarse gravel using implanted motion-sensing radio transmitters

James P McNamara* and Carter Borden†
Department of Geosciences, Boise State University, 1910 University, Dr. Boise, ID

Abstract:

Motion-sensing radio transmitters were implanted in cobbles (72–92 mm diameter) and placed in a stream in south-west Idaho for 43 days during a snowmelt period. The radios transmit different pulse rates depending on whether the rocks are at rest or in motion. Every 30 s, a datalogger samples the receiver and records the pulse rate of the transmitters. Such information can be used to assess numerous properties of particle transport that are beyond the capabilities of conventional tracking methods. Conclusions include: (i) rocks are more likely to move on rising hydrograph limbs than on falling hydrograph limbs; (ii) the average Shields' parameter is 0·046; (iii) rocks move only a fraction of the time between initial and final motion during an event; (iv) the distributions of motion and rest periods are best modeled by gamma functions rather than exponential, but the distributions approach exponential as the tails are trimmed. Copyright © 2004 John Wiley & Sons, Ltd.

KEY WORDS incipient-motion; bedload; radio-tracking

INTRODUCTION

Despite considerable progress in the science of bedload mechanics in recent decades, the ability to predict sediment transport rates in rivers remains poor, at best within an order of magnitude (Wilcock, 2001). Impediments to accurate transport prediction are many and include the spatial and temporal variability of bed material and the turbulent nature of stream flow. These factors interact to produce numerous complicated properties of bedload transport, such as variability in incipient motion (Buffington and Montgomery, 1997) and hysteresis (Reid *et al*., 1985; Kuhnle, 1992).

One approach to addressing the transport prediction problem is to understand bedload transport based on the properties of the motion of individual particles. Several particle tracing and tracking techniques have been developed to study numerous aspects of bedload movement and particle motion in gravel-bed streams (see review by Sear *et al*. (2000)). Most involve techniques of varying degrees of sophistication to locate tagged particles after significant flow events such as visually locating painted rocks (Ferguson and Wathen, 1998), finding magnetically tagged rocks with a metal detector (Butler, 1977; Schmidt and Ergenzinger, 1992; Ferguson and Wathen, 1998), and finding rocks implanted with radio transmitters (Chacho *et al*., 1989; Schmidt and Ergenzinger, 1992). These post-event techniques provide valuable information on properties such as particle travel distances (Hassan *et al*., 1992), spatial distribution of entrainment (Wilcock, 1997) and vertical mixing (Hassan *et al*., 1992). They provide little information, however, on the behaviour of particles when they are in transport.

Motion-sensing radio transmitters that traditionally have been used to study wildlife are now being used to study the motion of individual bedload particles (Chacho *et al*., 1989, 1994, 1996; Habersack, 2001). An

* Correspondence to: James P McNamara, Department of Geosciences, Boise State University, 1910 University Drive, Boise, ID, USA. E-mail: jmcnamar@boisestate.edu
† Present address: University of Idaho, Department of Civil Engineering, 800 Park Boulevard, Suite 200, Boise, Idaho 83712, USA

Received 15 October 2001
Accepted 9 May 2003

advantage of motion-sensing transmitters is that they allow for continual observation of particles. A problem, however, is that the particle size of the radio-rocks is limited to the length of the embedded transmitter so that smaller particle sizes of the bed are not monitored. Transmitters implanted in rocks send different signals to a receiver if the rock is stationary or in motion. Records of these signals, coupled with the water discharge and channel geometry data, enable insight into important bedload transport phenomena that is beyond the capabilities of conventional tracing and tracking techniques. For example, by simultaneously monitoring stream flow and the motion properties of individual particles, it is possible to determine the discharge when entrainment occurs and therefore improve estimates of forces at incipient motion. Furthermore, the ability to know the motion of individual particles during transport has enabled some of the first field tests of the ideas proposed by Einstein (1937) that particles move in a stochastic series of step and rest events (Chacho *et al.*, 1996; Habersack, 2001).

The purpose of this study is to investigate the movement of coarse gravel in a snowmelt-dominated mountain stream using motion-sensing radio-tracking techniques. Specifically, we investigate the motion and rest properties of individual particles with respect to rising and falling flows over the duration of the snowmelt period, and properties of particle behaviour during daily events including incipient motion, the duration of particle motion and the stochastic nature of motion and rest periods.

STUDY AREA

The Reynolds Creek Experimental Watershed (RCEW) (Figure 1) in the Owyhee Mountains of south-west Idaho is a field laboratory for the development and assessment of land management practices on western rangelands. The Northwest Watershed Research Center (NWRC), a research group of the United States Department of Agriculture (USDA), operates RCEW. Although extensive research has been conducted in many scientific disciplines within RCEW, bedload transport has received little attention. In 1974 and 1975, Johnson and others conducted studies evaluating the performance of the Helley-Smith sampler in measuring bedload transport rates in Reynolds Creek (Johnson *et al.*, 1977; Johnson and Hanson, 1976). Johnson *et al.* (1977) concluded that 20% of the sediment leaving the basin was in the form of bedload. Nearly all of the bedload movement occurs during the snowmelt period when stream flows are highest for the year.

The study reach begins approximately 400 m above the Tollgate Weir, elevation 1410 m, which drains 54·48 km^2 (Figure 1). The reach is classified as a plane-bed stream according to the Montgomery and Buffington (1997) scheme, is approximately 10 m wide and has a bed slope of 0·026. The d_{16}, d_{50} and d_{84} of the bed surface are 40 mm, 84 mm and 176 mm, respectively (Figure 2). Springtime hydrographs show a diurnal cycle related to snowmelt in the higher elevations. The Manning's roughness coefficient for a minor mountain stream with gravels, cobbles and few boulders ranges between 0·03 and 0·05 (Dingman, 1994).

METHODS

Five rocks (Table I) were implanted with Telonics IMP/210/L hermetically sealed transmitters of cylindrical dimensions 8·1 × 2·3 cm equipped with Telonics S6B motion sensors. Implant holes were bored into the rocks with a diamond bit and a drill press. The radio-rocks were painted bright yellow and placed in cross-section prior to the snowmelt period by tossing them into the creek and letting them settle into natural positions in the bed. The b-axes of the radio-rocks range between 76 and 92 mm, which closely match the range of d_{50} in the streambed (Figure 2). The straight, plane-bed reach with a relatively uniform grain-size distribution allowed for approximately equal chances of initial entrainment. The radio-rocks were occasionally located by tracking them with a Telonics portable directional antenna, receiver and signal strength meter to measure the transport distance. Four cross-sections and a longitudinal profile were surveyed between the starting location

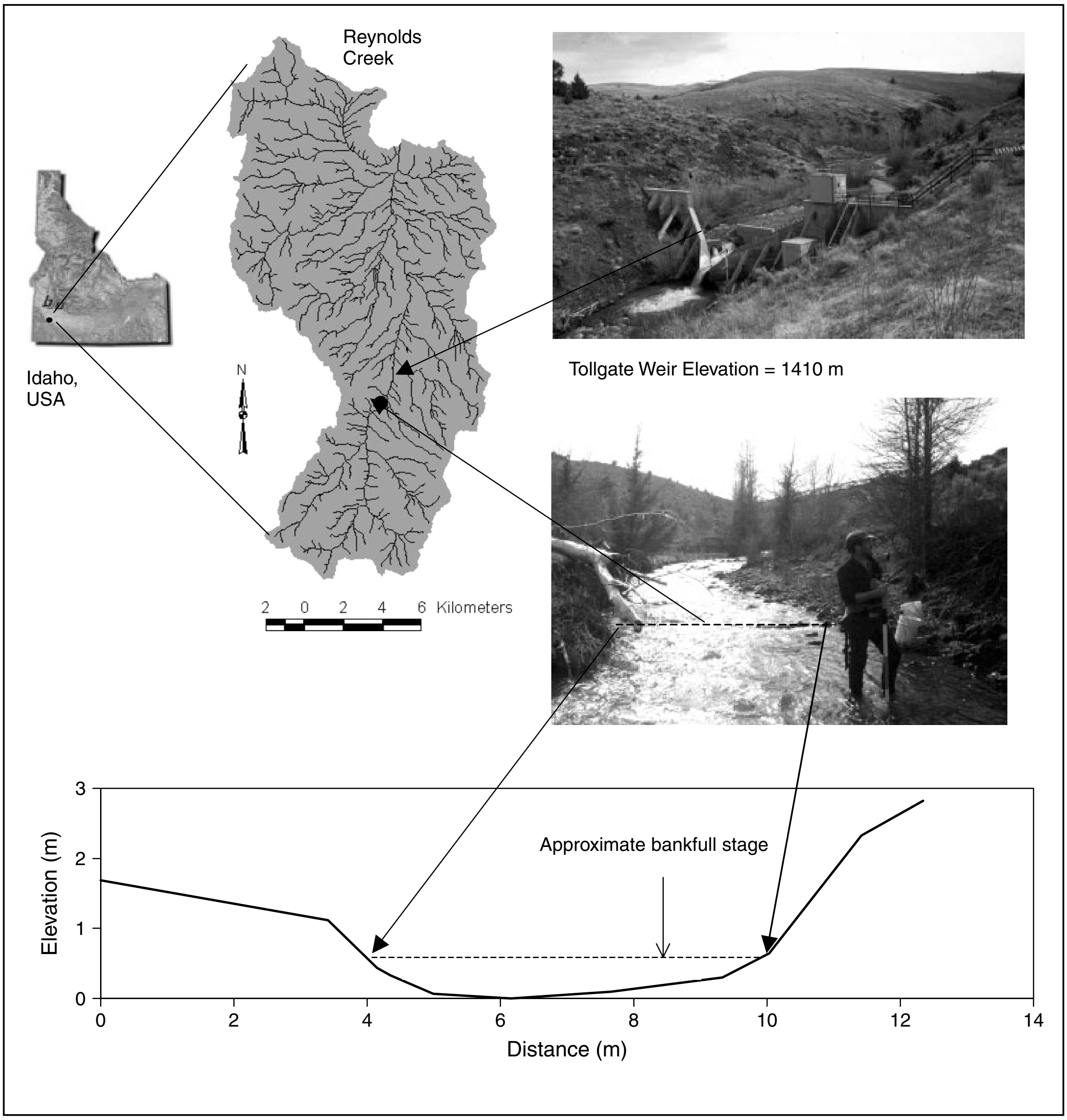

Figure 1. Study location in Reynolds Creek, south-west Idaho, USA. The study reach is approximately 400 m upstream of the tollgate weir

and the weir to obtain reach-averaged cross-section geometry for hydraulic calculations. The NWRC provided stream-flow discharge data in a 15-min time-series at the Tollgate weir (Pierson *et al.*, 2001).

Each motion-sensing transmitter sends pulses on a unique frequency at one preset pulse rate, or interpulse period, if the radio-rock is at rest and a different rate if the radio-rock is in motion. A mercury switch triggers the motion sensor from the resting pulse-rate to the motion pulse rate. Sensitivity tests showed that simple jarring the rock, as might happen to a rock in a streambed, does not trigger the switch. A rotation

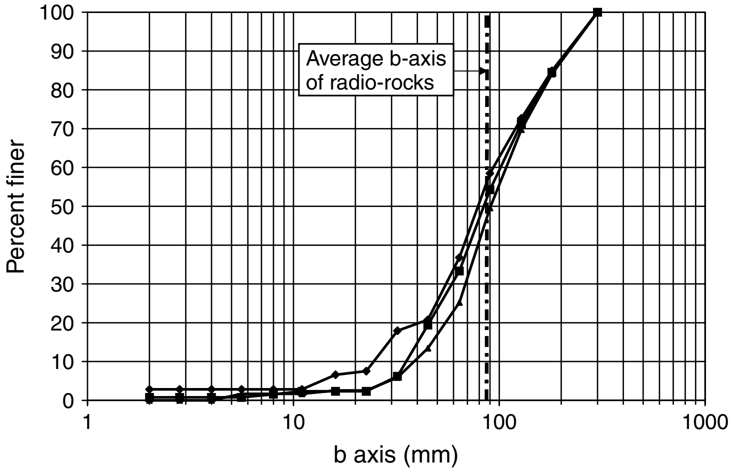

Figure 2. Surface grain-size distribution of three cross-sections in the Reynolds Creek study reach obtained by measuring approximately 100 randomly selected rocks in each cross-section. The dashed line represents the average *b* axis of the radio-rocks

Table I. Properties of radio-rocks

	Rock 858	Rock 863	Rock 867	Rock 903	Rock 947
a axis (mm)	144	142	120	144	116
b axis (mm)	88	76	92	88	88
c axis (mm)	84	62	64	68	64
Density (g/cm^3)	2·34	2·29	2·51	2·55	2·7

of approximately 1/4 turn, however, will trigger the switch. A receiver station is located on the bank about half way between the location of emplacement and the Tollgate Weir. The Telonics receiver station consists of an omni-directional RA-6B antenna, a TR-2 programmable receiver, a TS-1 scanner, a TDP-2 digital data processor and a Campbell Scientific CR10X datalogger. The scanner changes frequencies on the receiver at a user-defined time interval (5 s in this study). The receiver continually relays the pulse rate information from a transmitter to a digital data processor, which then displays the interpulse period being received in seconds. Current (0–1 milliampere) proportional to the interpulse period is sent to the datalogger and is converted to a voltage signal through a precision (1% tolerance) 100-ohm resistor. The datalogger samples the voltage drop across the resistor at defined time intervals. The resting and motion interpulse periods of the transmitters used in this study are approximately 1700 ms and 875 ms, respectively. The corresponding voltages for rest and motion periods are approximately 2500 and 1300 mV.

The datalogger initiates a sampling interval every 5 s by switching the frequency on the receiver. A 5-s sample interval includes a 2-s delay to allow the receiver to settle on the new frequency followed by a sample, another 2-s delay followed by another sample, then slightly less than a second before beginning again on a new frequency. With five motion-sensing transmitters and one beacon transmitter used as a marker in the output file it takes 30 s to cycle through the transmitters.

When a radio-rock moves, the pulse rate switches from the resting pulse rate to the motion pulse rate and remains at the motion pulse rate for a duration defined by the user, which was 30 s in this study to match the sample cycle. For example, if a rock moves just long enough to trigger the switch then stops, the radio transmits at the motion pulse rate for 30 s. A no-data period occurs when the sampled interpulse period does not match the rest or motion interpulse periods of the transmitter. This can occur if the receiver does not settle on the programmed frequency before the datalogger samples. The resulting data are a record for each rock every 30 s indicating if the rock moved or did not move during that period.

In RCEW, the diurnal fluctuations in stream flow during the snowmelt period create a predictable set of storms to investigate the movement of rocks during high stream-flow events. We analysed the rock motion properties during each stream-flow event by identifying the times and flow rates of initial motion and final motion, and by counting the number of motion and rest periods in between those times. It is possible that a rock can move through the recession of one stream-flow event and into the rise of the next. We base our analysis, however, on stream-flow events because it is a rather arbitrary decision to define the length of a rest period required to count as a new motion event.

RESULTS AND DISCUSSION

The stream began to rise steeply from snowmelt in the high elevations on day 102 (12 April) and diurnal fluctuations in stream-flow from daily snowmelt continued for approximately 2 months. The first rock motion occurred on day 106 (16 April). Four of the radio-rocks moved between 6 and 55 m over the duration of the study (Table II) in motion periods associated with most daily peak flows (Figure 3). During the snowmelt period, stream flow typically begins to rise each day near 1300 hours and peaks near 1900 hours. There were two periods of high activity separated by a low-flow period between days 123 (3 May) and 141 (21 May) in which little motion occurred (Figure 3). One rock moved only a few metres in the first couple days of the experiment then dropped behind a boulder and never moved again. This remaining analysis includes only those four rocks that moved throughout the study.

We analyse the motion properties of each rock in two ways. First, we investigate the occurrence of motion and rest periods over the entire study duration, paying particular attention to the distribution of motion periods on the rising and falling hydrograph limbs. Second, we investigate the properties of motion during individual daily flow events. Note that in the following discussions the term 'period' refers to a 30-s datalogger cycle.

Distribution of motion and rest periods during rising and falling flows

Each period between the time of first motion on day 106 (16 April) and final motion on day 149 (29 May) is counted as either a motion period, rest period, or no-data period for each of the four active rocks and

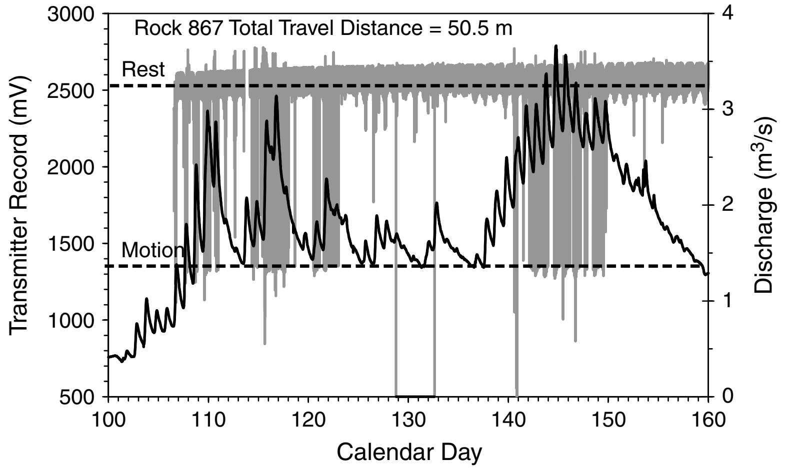

Figure 3. Example data from rock 867. The dark line represents the stream discharge (right-hand axis). The grey line represents the motion property of the rock (left-hand axis). The value of the left-hand axis is millivolts and represents the interpulse period of the transmitter. When the grey line is near 2500 mV the rock is at rest. When the grey line drops to near 1300 mV the rock is in motion

Table II. Counts, distributions and durations of motion, rest and no-data periods during rising, falling and total flows

Period		Rock 858 (travel distance, 7m)			Rock 867 (travel distance, 51m)			Rock 903 (travel distance, 22m)			Rock 947 (travel distance, 55m)		
		Rising limbs	Falling limbs	Total	Rising limbs	Falling limbs	Total	Rising limbs	Falling limbs	Total	Rising limbs	Falling limbs	Total
Counts	Motion	478	536	1014	3095	2694	5794	611	660	1271	8025	7150	15 175
	No data	2180	3840	6020	1121	1542	2730	2268	4250	6518	2144	3033	5177
	Rest	35 774	82 006	117 780	33 590	81 587	116 378	35 502	81 648	117 150	29 601	74 737	104 338
	Total	38 432	86 382	124 814	37 806	85 823	124 902	38 381	86 558	124 939	39 770	84 920	124 690
Distributions of occurrence	Motion	0·471	0·529	1·000	0·534	0·465	1·000	0·481	0·519	1·000	0·529	0·471	1·000
	No data	0·362	0·638	1·000	0·411	0·565	1·000	0·348	0·652	1·000	0·414	0·586	1·000
	Rest	0·304	0·696	1·000	0·289	0·701	1·000	0·303	0·697	1·000	0·284	0·716	1·000
	Total	0·308	0·692	1·000	0·303	0·687	1·000	0·307	0·693	1·000	0·319	0·681	1·000
Durations of occurence	Motion	0·012	0·006	0·008	0·082	0·031	0·046	0·016	0·008	0·010	0·202	0·084	0·122
	No data	0·057	0·044	0·048	0·030	0·018	0·022	0·059	0·049	0·052	0·054	0·036	0·042
	Rest	0·931	0·949	0·944	0·888	0·951	0·932	0·925	0·943	0·938	0·744	0·880	0·837
	Total	1·000	1·000	1·000	1·000	1·000	1·000	1·000	1·000	1·000	1·000	1·000	1·000

classified as occurring as either a rising or falling flow (Table II). As would be expected, rocks that moved the farthest had more motion periods. Table II contains the proportions of motion, rest and no-data, periods that occur during rising and falling flows, which are derived from Table II. For each rock, the rest periods were distributed between rising and falling limbs similarly to the durations of each hydrograph limb. However, the motion periods were nearly equally distributed between rising and falling limbs. For example, for rock 947, 53% of motion periods occurred on rising limbs and 47% of motion periods occurred on falling limbs, 28% of rest periods occurred on rising limbs and 72% of rest periods occurred on falling limbs. Thirty-two per cent of all periods occurred on rising limbs and 68% of all periods occurred on falling limbs. This is equivalent to saying that the stream was in a rising limb of a hydrograph 32% of the time.

The probability distributions of hourly discharge values during the study period for rising and falling limbs are nearly identical to each other (Table III). We can therefore directly compare the proportions of rest and motion periods with the durations of rising and falling flows. That the number of occurrences of motion periods was approximately the same on short-duration rising limbs as on long-duration falling limbs suggests that the radio-rocks were more likely to move on rising limbs than on falling limbs for equivalent flows.

This same conclusion is reached by investigating the durations during rising and falling flows that each rock spent in motion (Table II). For example, rock 947 was in motion during 20% of all rising flows and 8% of all falling flows. It was at rest during 74% of rising flows and 88% falling flows. Because the distributions of hourly discharges for rising and falling flows are nearly identical to each other, any given flow rate is therefore more likely to move rock 947 if it occurs on a rising limb than if it occurs on a falling limb. This observation is true for all four radio-rocks in the analysis. Each radio-rock was two to seven times more likely to move on rising hydrograph limbs than on falling hydrograph limbs.

Motion and rest properties during events

We define an event as a period of time in which stream flow experiences a discernable peak and motion of a tracer rock occurred in at least two motion periods separated by a rest period. Motion and rest properties were tabulated for each event, and the distributions of those properties for the entire set of daily events are summarized in Table IV. Here, we investigate incipient motion, the duration of motion and the stochastic nature of motion and rest periods.

Incipient motion. A particle in the bed moves when hydraulic lift and drag forces overcome the particle's resistance to motion (Dingman, 1984). Because lift and drag forces are difficult to measure in the field, it is a common task to calculate incipient motion as a result of the critical value of some hydraulic variable that is related to those forces such as shear stress, discharge or stream power (Dingman, 1984). The classic representation of incipient motion is in terms of critical shear stress as presented by Shields (1936)

$$\tau_{ci} = \theta_{ci}(\gamma_s - \gamma)d_i \qquad (1)$$

where τ_{ci} is the critical boundary shear stress required to move a particle in size class i with a diameter d_i, γ is the specific weight of water, γ_s is the specific weight of the particle and θ_{ci} is the critical dimensionless shear stress, or Shields' parameter. Equation (1) is conceptually a force balance equation where τ_{ci} represents the driving forces per unit area required to move a particle and $(\gamma_s - \gamma)d_i$ represents the forces per unit area that

Table III. Distribution of hourly stream-flow values, Q, for rising, falling-land all flow

	Q_{ave}	Q_{SD}	Q_{max}	Q_{min}	Q_{25}	Q_{75}
Falling flow	1·94	0·58	3·61	0·74	1·53	2·43
Rising flows	2·04	0·62	3·64	0·74	1·56	2·58
All flows	1·97	0·57	3·64	0·74	1·54	2·48

Table IV. Distribution of motion properties during individual events

Rock	Statistic	Hydrograph				Motion				Rest					No-data periods	Derived	
		Q_p	Q_i	Q_f	Total duration	Periods	Groups	Maximum duration	Average duration	Periods	Groups	Maximum duration	Minimum duration	Average duration		Motion factor	Shields' parameter, θ_c
858	Average	2·26	2·18	2·10	1669	48	26	5	1	1576	47	589	49	226	45	0·048	0·048
	SD	0·69	0·63	0·53	967	82	34	6	1	928	45	653	155	341	89	0·075	0·007
	CV	0·30	0·29	0·25	1	2	1	1	0	1	1	1	3	2	2	1·566	0·151
	Maximum	3·66	3·62	2·80	3086	367	143	19	3	2987	153	2207	675	1341	367	0·270	0·063
	Minimum	1·38	1·26	1·26	2	2	1	1	1	0	2	0	1	17	0	0·001	0·037
	Q_{25}	1·70	1·59	1·60	702	6	6	1	1	697	12	119	1	42	0	0·004	0·041
	Q_{50}	2·01	2·11	2·09	1879	13	10	2	1	1697	26	332	1	108	5	0·019	0·048
	Q_{75}	2·96	2·77	2·59	2362	47	28	7	2	2179	62	740	2	233	38	0·051	0·055
	n	41	24	24	21	21	21	21	21	21	21	21	21	21	21	16	24
867	Average	2·26	1·90	1·99	2076	182	62	47	3	1856	72	753	8	150	40	0·085	0·043
	SD	0·69	0·55	0·55	1197	211	60	111	6	1098	63	568	38	253	70	0·097	0·007
	CV	0·30	0·29	0·27	1	1	1	2	2	1	1	1	5	2	2	1·137	0·154
	Maximum	3·66	2·89	3·06	6075	731	213	413	33	5558	248	2180	218	1123	241	0·383	0·054
	Minimum	1·38	0·74	0·93	238	2	2	1	1	235	3	75	1	13	0	0·002	0·027
	Q_{25}	1·70	1·61	1·59	1155	14	14	1	1	944	16	299	1	25	0	0·010	0·040
	Q_{50}	2·01	1·67	1·86	2527	84	40	9	2	2021	55	694	1	43	1	0·062	0·041
	Q_{75}	2·96	2·40	2·46	2780	302	89	24	2	2534	106	991	1	134	38	0·137	0·049
	n	41	34	34	32	32	32	32	32	32	32	32	32	32	32	31	34
903	Average	2·26	2·07	1·98	2138	47	31	5	1	2023	64	660	26	209	71	0·024	0·047
	SD	0·69	0·61	0·57	1482	62	35	7	0	1408	63	508	93	289	86	0·030	0·007
	CV	0·30	0·29	0·29	1	1	1	1	0	1	1	1	4	1	1	1·237	0·155
	Maximum	3·66	3·00	3·07	8242	232	112	25	2	7860	214	1832	477	1074	234	0·105	0·057
	Minimum	1·38	0·96	0·93	19	2	2	1	1	17	3	17	1	13	0	0·001	0·032
	Q_{25}	1·70	1·62	1·55	1552	5	5	1	1	1548	12	297	1	34	3	0·004	0·042
	Q_{50}	2·01	1·97	1·79	2188	17	16	2	1	2013	60	558	1	46	18	0·012	0·046
	Q_{75}	2·96	2·63	2·56	2579	80	55	8	1	2435	81	878	6	236	135	0·029	0·054
	n	41	32	32	27	27	27	27	27	27	27	27	27	27	27	26	32

947	Average	2·26	1·88	1·86	2625	421	139	57	3	2133	149	635	3	75	62	0·160	0·045
	SD	0·69	0·48	0·57	1384	332	106	72	2	1192	109	575	13	276	61	0·110	0·006
	CV	0·30	0·26	0·30	1	1	1	1	1	1	1	1	4	4	1	0·692	0·131
	Maximum	3·66	2·92	3·12	8312	1079	512	313	7	7079	515	2266	78	1677	209	0·414	0·057
	Minimum	1·38	1·29	0·94	81	2	2	1	1	78	3	39	1	6	1	0·014	0·037
	Q_{25}	1·70	1·54	1·48	2070	115	62	12	2	1641	68	186	1	11	17	0·055	0·041
	Q_{50}	2·01	1·76	1·62	2694	318	116	27	3	2098	119	523	1	20	35	0·145	0·044
	Q_{75}	2·96	2·13	2·22	2945	773	195	70	4	2432	232	907	1	38	74	0·251	0·048
	n	41	39	39	36	36	36	36	36	36	36	36	36	36	36	36	39

Q_p, peak flow rate (m^3/s) during the stream-flow event; Q_i, flow rate (m^3/s) at the time of initial motion of the rock; Q_f, flow rate (m^3/s) at the time of final motion of the rock.
Total duration, the number of 30-s periods between the time of Q_i and the time of Q_f.
Periods, the number of 30-s periods during the total duration that the rock was in motion, at rest, or had no data.
Groups, the number of continuous motion or rest groups separated by at least one 30-s rest period.
Maximum duration, the number of 30-s periods in the longest motion or rest group.
Average duration, the average number of 30-second motion periods in all motion or rest groups.
Minimum duration, the number of 30-s motion periods in the shortest rest group.
Motion factor, motion periods divided by total duration.

resist motion. Because the lift and drag forces that actually move particles are not explicit in Equation (1), an empirical coefficient, θ_{ci}, is needed to account for the relationship between τ_{ci} and those forces. That relationship is complicated by several factors including particle shape, embedding, relative size, boundary roughness and the many ways in which turbulent flow imparts lift and drag forces on the particle.

To calculate τ_{ci}, it is necessary to assume a value of θ_{ci}. Shields reported that for fully turbulent flow, the value of the critical dimensionless shear stress for the median grain size in a streambed, θ_{c50}, of near-uniform grains is approximately 0·06. It is common practice, however, to assume that $\theta_{c50} = 0{\cdot}045$ after a reanalysis of Shields' original data by Gessler (1971). Buffington and Montgomery (1997) reported that in over 600 studies spanning eight decades Shields' parameter ranged between 0·03 and 0·086. The variability among those studies arises from many factors including bed properties, flow conditions and methods of estimation.

We calculate Shields' parameter for multiple events for each of the four radio-rocks by estimating parameters in Equation (1) from discharge values at initial motion and channel geometry information. The left-hand side of Equation (1) is equivalent to the boundary shear stress, τ, where

$$\tau = \gamma_w R\, S \tag{2}$$

and R is the hydraulic radius, γ_w is the specific weight of water and S is the slope of the water surface. Substitution of Equation (2) into Equation (1) yields

$$\gamma_w R\, S/(\gamma_p - \gamma_w)d_i = \theta_{ci} \tag{3}$$

Shields' parameter for the median bed material, θ_{c50}, is obtained through Equation (3) when $d = d_{50}$. The close match between the b axes of the radio-rocks and d_{50} of the bed surface validates this assumption (Figure 2). Shields' parameter is obtained by determining the hydraulic radius and slope at the time of motion. The slope is assumed to be constant in time and equal to the slope of the water surface at the time of the survey. An improved study of incipient motion should account for a changing slope with stage.

The flow rates at initial motion, Q_i, for each event (Table IV) are assumed to be the critical discharges, Q_c, to produce motion. Critical discharge is converted to a critical hydraulic radius through Manning's equation

$$Q_c = (1/n){R_c}^{2/3}S^{1/2}A_c \tag{4}$$

where n is Manning's roughness coefficient, S is the energy slope (assumed equal to the water surface slope), and A_c and R_c are the channel cross-section area (m^2) and the hydraulic radius (m) for the critical discharge. Manning's n was determined to be 0·05 by comparing physical properties of the stream to descriptions in a table of values found in Dingman (1994). One problem with this approach is that it is based on a reach average shear stress when in fact individual particles experience point-specific shear stresses. The use of reach average shear stress, however, is a common procedure because of the difficulties in measuring point-specific values.

The average flow at initial motion, Q_i, ranges between 1·88 m^3/s and 2·18 m^3/s, and the coefficients of variation and ranges of Q_i are similar among the four rocks (Table IV). These flows translate to average θ_{c50} values between 0·043 and 0·048 with an overall average of 0·046 (Table IV), which is similar to the commonly cited value reported by Gessler (1971). The minimum and maximum θ_{c50} are 0·027 and 0·063, respectively, compared with 0·03 and 0·086 reported by Buffington and Montgomery (1997). The range of Shields' parameter probably is related to using reach-average shear stresses in our calculations when each cobble actually experiences a range of stresses as it is trapped and exposed during its downstream travel. The distributions of θ_{c50} for each rock are bimodal (Table IV and Figure 4). This may reflect the influence of boulders and small steps in a predominately plane-bed reach. There are no significant differences between distributions of Q_i and Q_f.

Motion factors. The motion factors reported in Table IV indicate the proportion of time between initial and final motion within an event that the rocks were actually in motion. They are derived by dividing the motion

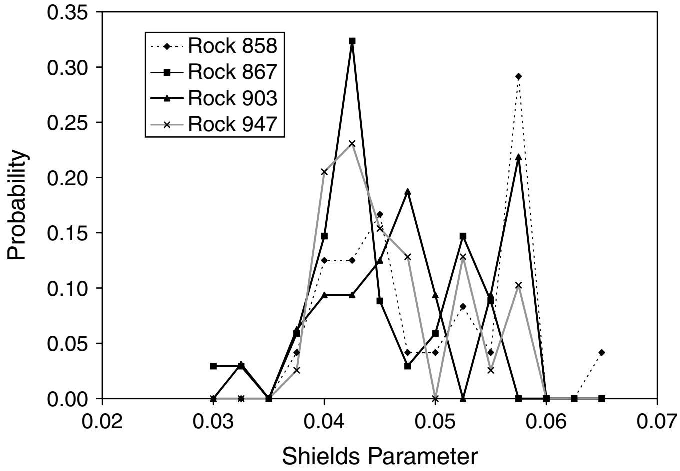

Figure 4. Probabilities for 0·0025 increments of Shields' parameter

periods by the total duration. The average motion factor for the four rocks ranged between 0·02 and 0·16. These averages exclude values of 1, which occur when a rock only moves during one period in a stream flow event. Chacho *et al.* (1994) reported a similar range. Habersack (2001) reported a motion factor for a braided stream in New Zealand of 0·027. That the motion factors are far less than 1 is consistent with the idea that once a rock is entrained motion occurs in a series of step and rest periods.

Stochastic nature of particle motion. We use the data underlying the distributions in Table IV to assess the stochastic nature of particle motion. A continuous set of motion or rest periods is called a motion or rest group. A comparison of maximum motion groups and maximum rest groups with their respective average values reveals highly skewed distributions (Table IV). Similar laboratory observations led Einstein (1937) to propose that once entrained, the transport of bedload is a stochastic process in which particles move along the bed in discrete steps separated by rest periods until final deposition. Einstein further hypothesized that the stochastic nature of step lengths and rest durations can both be described by exponential distributions. The probability density function for an exponential distribution is

$$f(x; \lambda) = \lambda e^{-\lambda x} \tag{5}$$

where x is the variable (either step length or rest duration) and λ is the inverse of $\bar{x}$.

Yang and Sayre (1971) showed that rest durations for sand in a flume follow an exponential distribution, but that a gamma distribution describes step lengths. The probability density function for a gamma distribution is

$$f(x; \alpha; \beta) = \frac{x^{\alpha-1} e^{-\frac{x}{\beta}}}{\beta^{\alpha} \Gamma(\alpha)} \tag{6}$$

where x is the variable, Γ () is a gamma function, α is the shape parameter of Γ (), and β is $\bar{x}$. It is important to note that when $\alpha = 1$, the gamma distribution becomes the exponential distribution. The parameters on the gamma distribution allow for more extreme tails than the exponential distribution allows.

Until radio-tracking techniques were imported from wildlife studies to bedload studies by Chacho *et al.* (1989), field investigations of the distributions of step lengths and rest durations were difficult and rare. Schmidt and Ergenzinger (1992) used single-frequency radio-tracers in coarse material in a step–pool mountain river to show that exponential distributions can explain both step lengths and rest durations. Chacho *et al.* (1994) were the first to use motion-sensing radio transmitters to investigate this problem and reported an exponential distribution of rest periods in a gravel bed river in Alaska. Habersack (2001) conducted the only other study using motion-sensing radio transmitters that we are aware of and reported an exponential distribution of rest periods and a gamma distribution of step lengths.

We use observations on motion duration to infer distributions of step lengths assuming that motion durations are linearly related to step lengths (Yang and Sayre, 1971). Visual inspection of Figure 5a and b reveals that gamma distributions give good fits to both motion and rest durations, whereas exponential distributions do not. The failure of the exponential distribution to model motion and rest durations arises from the extreme tails in both data sets. There are high numbers of one-period motion durations and long rest durations. This has important implications on how we distinguish between rest durations that are within events and those that separate events. For example, if we eliminate all rest durations greater than 10 min from the data set the distribution of rest durations becomes exponential.

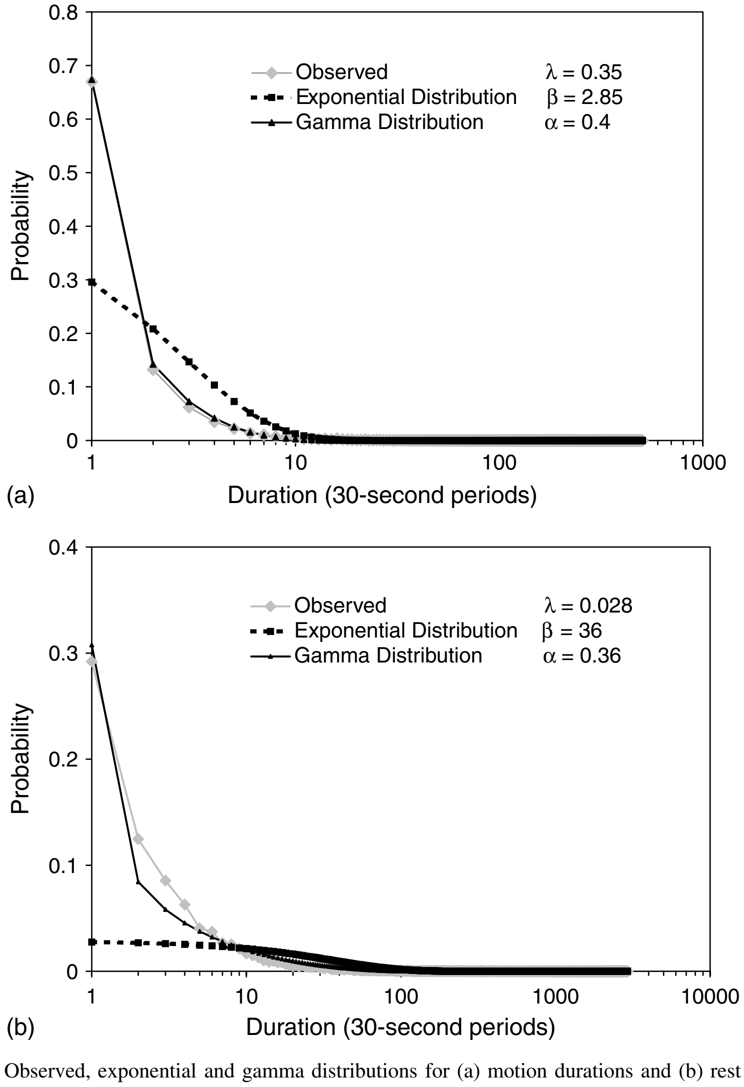

Figure 5. Observed, exponential and gamma distributions for (a) motion durations and (b) rest durations

Data quality

There are two primary issues concerning data quality. First, no-data periods accounted for 2·2% to 5·2% of all periods for the four rocks (Table IIa). A no-data period occurs when the voltage sampled by the datalogger does not correspond to either the motion or rest interpulse period of the transmitter. This problem can arise when the datalogger samples the signal processor before the receiver has settled on the current frequency. A solution is to spend more time on each frequency, and sample at the end of the interval. The 5-s sample interval used in this study was probably too short. Radio interference may also cause erroneous interpulse and no-data periods. Further, diurnal fluctuations occur in the voltage that the datalogger samples. These diurnal fluctuations probably result from the influence of daily temperature fluctuations on the performance of the crystal in the receiver, or on the resistor in the datalogger that converts current from the signal processor to voltage. Stream flow also rises and falls in diurnal cycles, which leads to similar cycles in motion properties. If the diurnal error is large enough, it may lead to difficulty in detecting actual motion events. A second data quality problem is the uncertainty of the magnitude of motion that occurs when the motion sensor is triggered. We do not know if the rocks simply rotate in place at times, or if there is actual downstream motion associated with each motion period.

CONCLUSIONS

Conclusions concerning the motion of coarse gravel bedload particles derived using motion-sensing radio transmitters include: (i) rocks are more likely to move on rising hydrograph limbs than on falling hydrograph limbs; (ii) the distribution of Shields' parameter is bimodal with an average value of 0·046; (iii) rocks move only a fraction of the time between initial and final motion during an event; (iv) and the distributions of motion and rest periods are best modelled by gamma functions rather than exponential functions, but both distributions approach exponential as the tails are trimmed.

Future work should focus on resolving data-quality issues related to the performance and sensitivity of the motion-sensing transmitters. Studies with many more tracers must be performed to strengthen the results concerning transport processes. However, the intense temporal sampling that is possible with the motion-sensing transmitters may offset the low number of physical samples.

ACKNOWLEDGEMENTS

This study was supported by a Faculty Research Grant from Boise State University. We thank Dr Charles Slaughter and James Fitzgerald for field assistance, and Dr John Buffington and two anonymous reviewers for insightful comments that substantially improved the manuscript.

REFERENCES

Buffington JM, Montgomery DR. 1997. A systematic analysis of eight decades of incipient motion studies, with spatial reference to gravel-bedded rivers. *Water Resources Research* **33**: 1993–2029.

Butler PR. 1977. Movement of cobbles in a gravel-bed stream during a flood season. *Geological Society of America Bulletin* **88**: 1072–1074.

Chacho EF, Burrows RL, Emmett WW. 1989. Detection of coarse sediment movement using radio transmitters. *XXIII Congress of the International Association for Hydraulic Research*, *August 1989, Ottawa, Ontario, Canada*. The National Research Council of Canada; B367–B373.

Chacho EF Jr, Burrows RL, Emmett WW. 1994. Monitoring gravel movement using radio transmitters. In *Hydraulic Engineering '94, Proceedings of the 1994 ASCE National Conference on Hydraulic Engineering*, *August 1994* Cotroneo GV, Rumer RR (eds), Buffalo, NY; 785–789.

Chacho EFJ, Burrows RL, Emmett WW. 1996. Motion characteristics of coarse sediment in a gravel bed river. *Sixth Federal Interagency Sedimentation Conference*, Vol. 2, Las Vegas, NV; 1–8.

Dingman SL. 1984. *Fluvial Hydrology*. W.H. Freeman: New York; 383 pp.

Dingman SL. 1994. *Physical Hydrology*. Prentice Hall: Upper Saddle River, NJ.

Einstein HA. 1937. *The bed load transport as probability problem*. Mitteilung der Versuchsanstalt für Wasserbau an der Eidgenössishen Technischen Hochschule: Zurich.

Ferguson RI, Wathen SJ. 1998. Tracer-pebble movement along a concave river profile: virtual velocity in relation to grain size and shear stress. *Water Resources Research* **34**: 2031–2038.

Gessler J. 1971. Beginning and ceasing of sediment motion. In *River Mechanics*, Shen HW (ed.). H.W. Shen: Fort Collins, CO; 7 : 1–7 : 22.

Habersack HM. 2001. Radio-tracking gravel particles in a large braided river in New Zealand: a field test of the stochastic theory of bed load transport proposed by Einstein. *Hydrological Processes* **15**: 377–391.

Hassan MA, Church M, Ashworth PJ. 1992. Virtual rate and mean distance of travel of individual clasts in gravel-bed channels. *Earth Surface Processes and Landforms* **17**: 617–627.

Johnson CW, Hanson CL. 1976. Sediment sources and yields from sage-brush rangeland watershed. *Third Federal Inter-agency Sedimentation Conference*, March 1976 Vol. 1, Denver, CO; 1–70–1–80.

Johnson CW, Engleman RL, Smith JP, Hanson CL. 1977. Helley–Smith bed load samplers. *Journal of the Hydraulics Division, Proceedings of the American Society of Civil Engineers* **103**: 1217–1221.

Kuhnle RA. 1992. Bed load transport during rising and falling stages on two small streams. *Earth Surface Processes and Landforms* **17**: 191–197.

Montgomery DR, Buffington JM. 1997. Channel-reach morphology in mountain drainage basins. *Geological Society of America Bulletin* **109**: 596–611.

Pierson FB, Slaughter CW, Cram ZK. 2001. Long-term stream discharge and suspended-sediment database, Reynolds Creek Experimental Watershed, Idaho, United States. *Water Resources Research* **37**: 2857–2861.

Reid I, Brayshaw AC, Frostick LE. 1985. The incidence and nature of bedload transport during flood flows in coarse-grained alluvial channels. *Earth Surface Processes and Landforms* **10**: 33–44.

Schmidt KH, Ergenzinger P. 1992. Bedload entrainment, travel lengths, step lengths, rest periods—studied with passive (iron, magnetic) and active (radio) tracer techniques. *Earth Surface Processes and Landforms* **17**: 147–165.

Sear DA, Lee MWE, Oakey RJ, Carling PA, Collins MB. 2000. Coarse sediment tracing technology for littoral and fluvial environments: a review. In *Tracers in Geomorphology*, Foster IDL (ed.). Wiley: Chichester; 21–55.

Shields A. 1936. Anwendung der aenlichkeitshmechanik und der turbulenzforschung auf die geschiebebewegung. Mitteilungen det Preussischen Versuchsanstalt fur Wasserbau und Schiffbau: Berlin, Germany.

Wilcock PR. 1997. Entrainment, displacement, and transport of tracer gravels. *Earth Surface Processes and Landforms* **22**: 128–1138.

Wilcock PR. 2001. The flow, the bed, and the transport: interaction in flume and field. In *Gravel-bed Rivers V*, Mosley MP (ed.). New Zealand Hydrological Society: Christchurch; 183–219.

Yang CT, Sayre WW. 1971. Stochastic model for sand dispersion. *Journal of the Hydraulics Division* **97**: 265–288.

